Robotica (2009) volume 27, pp. 147–159. © 2008 Cambridge University Press
doi:10.1017/S0263574708004578 Printed in the United Kingdom

Maximum load carrying capacity of mobile manipulators: optimal control approach

M. H. Korayem,* A. Nikoobin and V. Azimirad

Robotic Research Laboratory, College of Mechanical Engineering, Iran University of Science and Technology, Tehran, Iran

(Received in Final Form: March 19, 2008. First published online: April 28, 2008)

SUMMARY

In this paper, finding the maximum load carrying capacity of mobile manipulators for a given two-end-point task is formulated as an optimal control problem. The solution methods of this problem are broadly classified as indirect and direct. This work is based on the indirect solution which solves the optimization problem explicitly. In fixed-base manipulators, the maximum allowable load is limited mainly by their joint actuator capacity constraints. But when the manipulators are mounted on the mobile bases, the redundancy resolution and nonholonomic constraints are added to the problem. The concept of holonomic and nonholonomic constraints is described, and the extended Jacobian matrix and additional kinematic constraints are used to solve the extra DOFs of the system. Using the Pontryagin's minimum principle, optimality conditions for carrying the maximum payload in point-to-point motion are obtained which leads to the bang-bang control. There are some difficulties in satisfying the obtained optimality conditions, so an approach is presented to improve the formulation which leads to the two-point boundary value problem (TPBVP) solvable with available commands in different softwares. Then, an algorithm is developed to find the maximum payload and corresponding optimal path on the basis of the solution of TPBVP. One advantage of the proposed method is obtaining the maximum payload trajectory for every considered objective function. It means that other objectives can be achieved in addition to maximize the payload. For the sake of comparison with previous results in the literature, simulation tests are performed for a two-link wheeled mobile manipulator. The reasonable agreement is observed between the results, and the superiority of the method is illustrated. Then, simulations are performed for a PUMA arm mounted on a linear tracked base and the results are discussed. Finally, the effect of final time on the maximum payload is investigated, and it is shown that the approach presented is also able to solve the time-optimal control problem successfully.

KEYWORDS: Maximum payload; Mobile manipulator; Path planning; Optimal control; Indirect method; Pontryagin; Redundancy.

* Corresponding author. E-mail: HKorayem@iust.ac.ir

1. Introduction

Fixed-based manipulators, currently used in applications, have limited workspace. But some applications need to carry loads between two long-distance positions, i.e., in construction, farming, forestry, military, and hazardous work sites, such as nuclear power plants or chemical production plants.[1–2] For such dangerous or unfeasible tasks, mobile manipulators are an ideal choice. They have a compact structure, large workspace, and high maneuverability and are cost-effective. One of the main usages of mobile manipulators is handling heavy loads from one place to another. Therefore, finding the full-load motion between the two given points in workspace can maximize the productivity and economic usage of these type of robots.

End-effector motion is a superposition of the base and the manipulator motions in mobile manipulators. Moreover, the addition of base and manipulator degrees of freedom causes the overall system to have extra degrees of freedom in its motion. Therefore, there may exist infinite solutions for motion planning of the system between two given end points. These extra DOFs can be used to accomplish one or more additional tasks besides the payload maximization purpose. Therein, the maximum payload motion of the redundant manipulator is given as a primary task and the subtasks can be achieved by choosing the proper constraint functions. The arbitrary subtasks can be considered as the limitation of workspace, avoidance of singularities or obstacles, or optimization criteria. Seraji presented an online approach for motion control of mobile manipulators using augmented Jacobian matrices.[3] He used additional kinematic constraints for redundancy resolution to be met for the manipulator configuration.

The maximum allowable load (MAL) of a manipulator is often defined as maximum payload that the manipulator can repeatedly lift in its fully extended configuration.[4] If the end-effector trajectory is prespecified, the MAL would be defined as the maximum value of load which a robot manipulator is able to carry on it.[4] Finding the maximum payload which a manipulator can carry between given initial and final position of the end-effector is also another way of obtaining the MAL. In this case, finding the maximum payload and corresponding optimal path is formulated as a trajectory optimization problem.[5] For finding the MAL of mobile manipulators, researchers are faced with a path-planning problem. Due to the extra DOFs and nonholonomic constraints, path-planning problem of mobile manipulators is a challenging and complicated task and has received

considerable attention in recent years. Generally, the problem of motion planning becomes quite complex and requires specific schemes for its treatment. Two main families for solving this problem can be distinguished: direct and indirect methods.[6,7]

Direct methods are based on a discretization of dynamic variables (states, controls) leading to a parameter optimization problem. Then, linear optimization,[5] nonlinear optimization,[8] evolutionary,[9] or classical stochastic techniques[10] are applied to obtain optimal values of the parameters. In most of the previous works dealing with path planning of mobile manipulators, the direct methods are employed, and often the Spline or polynomial functions are used as the motion profiles.[11,12] Wang *et al*. have solved the optimal control problem using the B-Spline functions in order to determine the maximum payload of a fixed-base manipulator.[8] The basic idea of this work is to parameterize the joint trajectories by the use of B-Spline functions, and tuning the parameters in a nonlinear optimization until a local minimum that satisfies the constraints is achieved. A weak point of this method is limiting the solution to a fixed-order polynomial. Another difficulty arises from the complexity of differentiating torques with respect to joint parameters and payload due to their constraints and discontinuity.

Iterative linear programming (ILP) is another direct technique, in which the trajectory optimization problem is converted into a liner programming problem. The first formulation of this method for a simple robot manipulator is presented by Wang and Ravani.[5] Korayem and Ghariblu used ILP method for the MAL calculation of mobile manipulators.[13,14] In these papers,[13–16] the MAL for mobile manipulators are determined subject to both actuator and redundancy constraints. For motion planning and redundancy resolution, additional constraint functions and the augmented Jacobian matrix are used, while a typical DC motor speed–torque characteristics curve is used to model the actuator constraints. The linearizing procedure in ILP method and its convergence is a challenging issue, especially when the nonlinear terms are large. As it can be seen from the simulation results,[13] the final boundary conditions are not satisfied exactly and the end-effector does not place in desired goal point. Generally, direct methods result in approximate solution of the problem. They are exhaustively time-consuming and quite inefficient due to the large number of parameters involved, especially for systems with a large number of DOFs.[17]

On the other hand, indirect method is based on Pontryagin maximum principle (PMP),[18] which solves the optimal control problem exactly. It was first used to solve the minimum time motion problems along the specified paths. Then, it was extended to handle free motions as well.[19,20] PMP is also used to treat directly the optimal dynamic motion-planning problem.[21] The optimality conditions for transfer modalities are expressed as a set of differential equations. This boundary values problem is solved by specific numerical techniques, such as shooting or relaxation methods. This method is widely used as a powerful and efficient tool in analyzing the nonlinear systems and path planning of different types of systems.[19–25] Mohri *et al*. have used indirect method for trajectory planning of mobile manipulators. They have proposed an approach to find the optimal path for both mobile base and manipulator links in order to achieve the minimum effort trajectory in point-to-point motion.[26] In the next works they have applied this method for trajectory planning of mobile manipulators with end-effector's specified path.[27,28] To solve the problem, all the states are considered as the design parameters and they have used a hierarchical gradient method which synthesizes the gradient function in a hierarchical manner based on the order of priority.

In this paper, determining the MAL of mobile manipulators between two given points is solved by using the indirect solution of optimal control problem. The extra DOFs arose from base mobility are solved using the additional constraint functions and the augmented Jacobian matrix, so the formulation and solution algorithm presented in refs. [26]–[28] will not be applicable here. Using the Pontryagin's minimum principle, optimality conditions for carrying the maximum payload in point-to-point motion are derived. The obtained conditions lead to a bang-bang control. The main challenge of this method is solving the obtained TPBVP, so formulation is improved and an algorithm is developed to convert the optimization problem into a standard form of TPBVP solvable with bvp4c commands in MATLAB. In order to verify the proposed method, simulations are performed for a two-link planar manipulator mounted on a differentially driven mobile base used in ref. [13]. Another simulation for a PUMA arm mounted on a linear tracked base is performed and it is shown how to obtain the various maximum payload trajectories via changing the objective functions. In the last case study, the effect of final time on the maximum payload value is studied, and it is shown that the method presented is also applicable for solving the time-optimal control problem efficiently.

2. Kinematic and Dynamic Modeling

2.1. Kinematic modeling and redundancy resolution

We denote q the generalized coordinates of the mechanical system as $q = [q_1, \ldots, q_n] = [q_b, q_m]$, where $q_b = q_1, \ldots, q_{n_b}$ is the base configuration space vector, $q_m = q_{n_b+1}, \ldots, q_n$ is the manipulator space vector, n_b is the number of mobile base DOFs, n_m is the number of manipulator DOFs, and $n = n_m + n_b$ is the overall system of degrees of freedom. By considering $X = [x, y, z]^T$ as the end-effector position in the world reference frame RF_w, the end-effector velocity of the mobile manipulator can be determined as

$$\dot{X} = J\dot{q}, \tag{1}$$

where $J = (J_b, J_m)$ and $\dot{q} = (\dot{q}_b, \dot{q}_m)^T$. $\dot{X} \in R^m$ denotes the end-effector velocity with respect to the RF_w and $\dot{q} \in R^n$ is the joints velocity vector. If the end-effector degrees of freedom in Cartesian space are denoted by m and mobility plus manipulation DOFs of the system by n, it is well known that in most mobile manipulator systems, we have $n > m$. As a result, the system has kinematic redundancy or extra degrees of freedom on its motion equal to $R = n - m$. There are different methods for redundancy resolution of robotic systems. Some of these methods are based on an

https://doi.org/10.1017/S0263574708004578 Published online by Cambridge University Press

optimization criterion, such as overall torque minimization, minimum joint motion, and so on. But there is a well-known method that applies additional suitable kinematic constraint equations to system dynamics and results in simple and online coordination of the mobile manipulator during the motion. This method borrows from the extended Jacobian matrix concept.[3,29,30]

Generally, the mobile manipulator may be subject to number of either holonomic or nonholonomic constraints. If the number of nonholonomic constraints of the system is denoted by c, the generalized form of these constraint equations is

$$J_c\,\dot{q} = 0, \tag{2}$$

where $\dot{q} \in R^n$ is the time derivative of motion variable vector and $J_c \in R^{c\times n}$ is the corresponding coefficient. On the other hand, the holonomic constraints have the general form $X_z = G(q)$ and differentiating it with respect to time gives

$$\dot{X}_z = J_z\dot{q}, \tag{3}$$

where $J_z \in R^{r\times n}$ is the corresponding coefficient and X_z is the vector of additional kinematic constraints as a function of system variables. As mentioned before, the extended Jacobian matrix technique can be used for redundancy resolution. Therefore, R extra degrees of freedom can be solved using c nonholonomic constraints and r holonomic constraints. By the other means for solvability, r additional functions must be applied to relate joint vectors to each other where $r = R - c$. By combining Eqs. (1), (2), and (3), the kinematic equation of mobile manipulators becomes

$$[\dot{X} \quad \dot{X}_z \quad 0]^T = [J \quad J_z \quad J_c]^T\dot{q}. \tag{4}$$

Here $J_a = (J, J_z, J_c)^T$ is named the augmented Jacobian matrix. However, as explained by Seraji [3], if r additional user-specified constraints are selected properly, then J_e would be nonsingular or $\mathrm{Det}(J_e) \neq 0$. These systems can be kinematically evaluated as if they were nonredundant. At this condition, the joint velocity and acceleration vectors are found as below:

$$\dot{q} = J_a^{-1}[\dot{X} \quad \dot{X}_z \quad 0]^T \tag{5}$$

$$\ddot{q} = J_a^{-1}\lfloor[\ddot{X} \quad \ddot{X}_z \quad 0]^T - \dot{J}_a\dot{q}\rfloor. \tag{6}$$

2.2. Dynamic modeling

Consider an n DOFs mobile manipulator with generalized coordinates $q = [q_i], i = 1, 2, \ldots, n$, and a task described by m task coordinates r_j, $j = 1, 2, \ldots, m$ with $m < n$. By applying r holonomic constraints and c nonholonomic constraints to the system, $r + c$ redundant DOFs of the system can be directly determined. Therefore, m DOFs of the system remains to accomplish the desired task. As a result, we can decomposed the generalized coordinate vector as $q = [q_r \quad q_{nr}]^T$, where $q_r \in R^{r+c}$ is the redundant generalized coordinates vector determined by applying the constraints and $q_{nr} \in R^m$ is the remaining generalized coordinate vector. The system dynamics can also be decomposed into two parts: one is corresponding to a redundant set of variables, q_r, and another is corresponding to a nonredundant set of them, q_{nr}. That is,

$$\begin{bmatrix} U_r \\ U_{nr} \end{bmatrix} = \begin{bmatrix} M_{r,r} & M_{r,nr} \\ M_{r,nr} & M_{nr,nr} \end{bmatrix}\begin{bmatrix} \ddot{q}_r \\ \ddot{q}_{nr} \end{bmatrix} + \begin{bmatrix} C_r + G_r \\ C_{nr} + G_{nr} \end{bmatrix}, \tag{7}$$

where $M \in R^{n\times n}$ is the inertia matrix, $C \in R^n$ is the Coriolis and centrifugal forces, and $G \in R^n$ is the vector of gravity force, respectively. Considering the row associated with nonredundant part leads to

$$U_{nr} = A\ddot{q}_{nr} + B, \tag{8}$$

where $A = \hat{M}_{nr,nr}$, $B = \hat{M}_{r,nr}\ddot{q}_r + \hat{C}_{nr} + \hat{G}_{nr}$, $\hat{M}_{nr,nr} = M_{nr,nr}(t, q_r, q_{nr})$, $\hat{M}_{r,nr} = M_{r,nr}\ (t, q_r, q_{nr})$, $\hat{C}_{nr} = C_{nr}(t, q_r, \dot{q}_r, q_{nr}, \dot{q}_{nr})$, and $\hat{G}_{nr} = G_{nr}(t, q_r, q_{nr})$. Using redundancy resolution, q_r will be obtained as a known vector in terms of the time (t). Therefore A is obtained as a function of t and q_{nr}, and B as a function of t, q_{nr}, and $\dot{q}_{nr}$. $\hat{M}_{r,nr}$, $\hat{M}_{nr,nr}$, and $\hat{G}_r$ are the functions of t and q_r, and $\hat{C}_{nr}$ is the function of t, q_{nr}, and $\dot{q}_{nr}$. By defining the state vector as

$$X = [X_1 \quad X_2]^T = [q_{nr} \quad \dot{q}_{nr}]^T, \tag{9}$$

Eq. (8) can be rewritten in state space form as

$$\dot{X} = [\dot{X}_1 \quad \dot{X}_2]^T = [X_2 \quad N(X) + Z(X)U], \tag{10}$$

where $N \in R^m$ and $Z \in R^{m\times m}$. Then optimal control problem is to determine the position and velocity variable $X_1(t)$ and $X_2(t)$, and the joint torque $U(t)$ such that we optimize a well-defined performance measure when the model is given in Eq. (10).

3. Optimality Conditions for Carrying the Maximum Payload

Let Ω be the set of the admissible control torques. The optimization problem is to find control $U(t) \in \Omega$ and payload m_p, so that the manipulator in Eq. (10) can carry maximum payload from an initial configuration to a final motion target. Therefore, the objective function that must be minimized is defined as

$$\underset{U(t),\, m_p}{\text{Minimize}}\ J_0 = -\frac{1}{t_f}\int_0^{t_f} m_p dt, \tag{11}$$

where m_p is the payload value, t_f is the final time, and the objective function will be equal to $-m_p$. So minimizing the objective function leads to maximizing the payload value. For the maximum payload problem, the state departing from initial conditions

$$X_1(0) = X_{10}, \quad X_2(0) = X_{20} \tag{12}$$

must reach the final conditions

$$X_1(t_f) = X_{1f}, \quad X_2(t_f) = X_{2f} \tag{13}$$

https://doi.org/10.1017/S0263574708004578 Published online by Cambridge University Press

in such a way that the maximum payload can be carried. The control forces are bounded as

$$U_i^- \le U_i \le U_i^+, \tag{14}$$

so according to the Pontryagin's minimum principle, the optimal solution (indicated here by *) must satisfy the following conditions:

$$\dot{X}^* = \partial H/\partial \psi, \tag{15}$$

$$\dot{\psi}^* = -\partial H/\partial X, \tag{16}$$

$$H(X^*, U^*, \psi^*, m_p^*) \le H(X^*, \psi^*, \bar{U}, \bar{m}_p) \tag{17}$$

for all time $t \in [t_0 \;\; t_f]$, where U^* is optimal control, m_p^* is maximum payload, $\bar{U}$ is all admissible control, and $\bar{m}_p$ is all admissible payload. The Hamiltonian $H(X, \psi, U, m_p)$ is defined as

$$\begin{aligned} &H(X, U, \psi, m_p) \\ &= -m_p/t_f + \psi_1^T X_2 + \psi_2^T [N(X, m_p) + Z(X, m_p)U], \end{aligned} \tag{18}$$

where $\psi = [\psi_1^T \;\; \psi_2^T]^T$ is the vector of costates. Equation (17) shows that optimal solution must minimize the Hamiltonian. Here, m_p and U are two independent parameters that must be determined to minimize the Hamiltonian function, so the following conditions must be satisfied:

$$\frac{\partial H}{\partial U} = 0, \tag{19}$$

$$\frac{\partial H}{\partial m_p} = 0. \tag{20}$$

Equation (20) leads to an algebraic equation which must be fulfilled for all $t \in [t_0 \;\; t_f]$. Since Hamiltonian is a linear function of U, condition (19) does not provide any useful relation between the controls and the states. So, in order to determine the optimal control law, substituting Eq. (18) into Eq. (17) gives

$$\begin{aligned} &-m_p^*/t_f + \psi_1^{*T} X_2^* + \psi_2^{*T} [N(X^*, m_p^*) + Z(X^*, m_p^*)U^*] \\ &\quad \le -\bar{m}_p/t_f + \psi_1^{*T} X_2^* + \psi_2^{*T} [N(X^*, \bar{m}_p) \\ &\quad + Z(X^*, \bar{m}_p)\bar{U}]. \end{aligned} \tag{21}$$

For a specified payload m_p, Eq. (21) reduces to

$$\psi_2^{*T} Z(X^*)U^* \le \psi_2^{*T} Z(X^*)\bar{U} \tag{22}$$

for all admissible controls $\bar{U}$ and for all $t \in [t_0 \;\; t_f]$. This equation states that the term $\psi_2^{*T} Z(X^*)\bar{U}$ must be minimized with respect to any control $\bar{U}$. It forces the control $\bar{U}$ to take its extremal values. Since the components of the controls are independent of each other, the optimal controls U_i to satisfy Eq. (21) must be assumed as

$$U_i = \begin{cases} U_i^+ & \text{for } \psi_2^T Z_i(X) < 0 \\ U_i^- & \text{for } \psi_2^T Z_i(X) > 0 \end{cases}. \tag{23}$$

Here $Z_i(X)$ is the ith column of matrix $Z(X)$. The function $G_i = \psi_2^T Z_i(X)$ is called the switch function corresponding to the control U_i. This type of control (23) is referred to as bang-bang control. The controls take their extremal values throughout the whole motion to minimize the objective function.

The actuators that are commonly used for medium- and small-sizes manipulators are the permanent magnet DC motor. The torque speed characteristic of such DC motors may be represented by the following linear equation [4]:

$$\begin{aligned} U^+ &= K_1 - K_2 X_2 \\ U^- &= -K_1 - K_2 X_2, \end{aligned} \tag{24}$$

where $K_1 = [\tau_{s1} \;\; \tau_{s2} \cdots \tau_{sm}]^T$, $K_2 = \text{dig}[\tau_{s1}/\omega_1 \cdots \tau_{sm}/\omega_m]$, τ_s is the stall torque, and ω is the maximum no load speed of the motor.

Here, we have $4m$ differential equations given in Eqs. (15), (16), and one algebraic equation given in Eq. (20), to determine the $4m$ state and costate variables, and one payload value. The set of differential equations (15) and (16), the requirements (20) and (23), and the boundary conditions (12) and (13) construct a class of two-point boundary value problem. In this formulation, some difficulties arise from Eq. (20) and control law (23). In Eq. (23), when $\psi^T Z_i(X) = 0$ for a period of time, the PMP is not able to define any optimal control. If the switch functions G_i are zero at individual points only, the sign of the control changes immediately and a very significant variation takes place in control law, which leads to infinite jerk in system. The other difficulty is due to the algebraic equation (20). It makes the solution of TPBVP very difficult and time-consuming, so that the convergence to the optimal solution hardly takes place. Also because of the presence of algebraic equation in TPBVP, it is not possible to use the available commands in different software provided to solve the boundary value problems.

In order to overcome the above-mentioned difficulties, in the next section, the formulation presented is improved to convert the optimization problem into a standard form of TPBVP, and then an algorithm is proposed to determine the maximum payload trajectory.

4. Improved Formulation for Maximum Payload Calculation

4.1. Necessary condition for optimality

The basic idea to improve the formulation is to find the optimal path for a specified payload, and then maximum payload is obtained via an iterative algorithm. For the sake of this, the following objective function is considered:

$$\underset{U(t)}{\text{Minimize}} \; J_0 = \int_{t_0}^{t_f} L(X, U)\, dt, \tag{25}$$

where

$$L(X, U) = \frac{1}{2} \|X_1\|_{W_1}^2 + \frac{1}{2} \|X_2\|_{W_2}^2 + \frac{1}{2} \|U\|_R^2. \tag{26}$$

Integrand $L(.)$ is a smooth, differentiable function in the arguments, $||X||_K^2 = X^T K X$ is the generalized squared norm,

https://doi.org/10.1017/S0263574708004578 Published online by Cambridge University Press

W_1 and W_2 are symmetric, positive semidefinite $(m \times m)$ weighting matrices, and R is symmetric, positive definite $(m \times m)$ matrices. The objective function specified by Eqs. (25) and (26) is minimized over the entire duration of the motion. The designer can decide on the relative importance among the angular position, angular velocity, and control effort by the numerical choice of W_1, W_2, and R that can also be used to convert the dimensions of the terms to consistent units.

According to the PMP, the following conditions must be satisfied:

$$\dot{X} = \partial H/\partial \psi, \quad \dot{\psi} = -\partial H/\partial X, \quad 0 = \partial H/\partial U, \tag{27}$$

where the Hamiltonian function is defined as

$$H(X, U, \psi) = 0.5\big(\|X_1\|^2_{W_1} + \|X_2\|^2_{W_2} + \|U\|^2_R\big) + \psi_1^T X_2 + \psi_2^T [N(X) + Z(X)U]. \tag{28}$$

So, according to Eq. (27), the optimality conditions can be obtained by differentiating the Hamiltonian function with respect to states, costates, and control as follows:

$$[\dot{X}_1 \quad \dot{X}_2]^T = [X_2 \quad N(X) + Z(X)U]^T, \tag{29}$$

$$[\dot{\psi}_1 \quad \dot{\psi}_2]^T = -[\partial H/\partial X_1 \quad \partial H/\partial X_2]^T, \tag{30}$$

$$RU + Z^T \psi_2 = 0. \tag{31}$$

The control values are limited with upper and lower bounds, so using Eq. (31), the optimal control is given by

$$U = \begin{cases} U^+ & -R^{-1}Z^T\psi_2 > U^+ \\ -R^{-1}Z^T\psi_2 & U^- < -R^{-1}Z^T\psi_2 < U^+ \\ U^- & -R^{-1}Z^T\psi_2 < U^- \end{cases}. \tag{32}$$

The bounds on the control input, $U^-$and U^+, can be substituted from Eq. (24). As it can be seen, the optimal control (32) does not have the problems mentioned for bang-bang control (23). In this formulation, for a specified payload value, $4m$ differential equations given in Eqs. (29) and (30) are used to determine the $4m$ state and costate variables. The set of differential equations (29) and (30), the control law (32), and the boundary conditions (12) and (13) construct a standard form of TPBVP, which is solvable with available commands in different software, such as MATLAB, C++, or FORTRAN.

4.2. Maximum payload calculation

The above equations represent three relation sets: (i) the dynamical model, Eqs. (29) and (30), (ii) the optimality condition, Eqs. (32) and (24), and (iii) the split boundary condition, Eqs. (12) and (13). These conditions specify a two-point boundary value problem which can be solved numerically. An iterative algorithm for computing a solution of this problem can be constructed by satisfying any two of the three conditions in each iteration. Then the algorithm will be repeated on the third condition awaiting the desired degree of accuracy. Here, substituting Eqs. (32) and (24) into Eqs. (29) and (30) establishes a set of $4m$ ordinary differential equations in terms of the state and costate variables (X, ψ), while Eqs. (12) and (13) describe $4m$ boundary value conditions in which $2m$ of them are defined at $t = t_0$, and other $2m$ of them at $t = t_f$. The algorithm iterates on the initial values of the costate until the final boundary conditions are satisfied. To put it another way, the following relation must be fulfilled in TPBVP solving:

$$\frac{1}{2}\|X_1(t_f) - X_{1f}\|^2_{W_p} + \frac{1}{2}\|X_2(t_f) - X_{2f}\|^2_{W_v} \le \varepsilon, \tag{33}$$

where $\varepsilon \ll 1$ is solution accuracy. $X_f$is the vector of desired boundary conditions at $t = t_f$ and $X(t_f)$ is the vector of calculated states values at $t = t_f$ per costate initial value obtained in TPBVP solution. Relative importance of position and velocity errors of each joint can be specified via choosing the component of W_p and W_v. For a known payload, the obtained equations are in the standard form of TPBVP which bvp4c command in MATLAB is used to solve it.

Up to now we suppose that the payload value is known and the solution of optimal control problem was obtained. Now, by using the solution of obtained TPBVP, an algorithm is presented in Fig. 1 in order to find the maximum payload. In this algorithm, e is the accuracy at maximum payload calculation and s is the iterations number. With the aid of this algorithm, the maximum payload for the supposed penalty matrices can be found. The solution method is based on increasing the payload from its minimum value, $m_{p\min}$, until the maximum payload value can be found. The solution algorithm presented has two loops. The loop index (i) increases the payload at each iteration, while the other one (k) adjusts the jump interval. Therefore, the accuracy in payload calculation is guaranteed as well as the approaching rate to final answer.

Desired accuracy ε in TPBVP solution for $m_p \le m_{p\max}$ is achievable, thus Eq. (33) is satisfied and payload increases in each step until the payload value becomes lager than its maximum value $(m_p > m_{p\max})$. At this condition, Eq. (33) will not be satisfied, because for carrying the payload more than $m_{p\max}$, the torque more than their limits is required. But it is impossible, because the torque constraints are satisfied at each iteration in TPBVP solution. Consequently, the boundary conditions at final time could not be satisfied and as soon as payload value becomes larger than $m_{p\max}$, the error value becomes large significantly. Thus the other loop (k) is acted, payload decreases, and the jump interval becomes smaller in loop (i) until the maximum payload be obtained with the accuracy e.

The formulation presented in Section 4.1 and the proposed algorithm in Fig. 1 can also be used for solving the time-optimal control problem. In this case, algorithm iterates on final time t_f instead of payload value m_p. By considering the maximum final time $t_{f\max}$, in each step t_f is decreased until the minimum time duration can be found.

5. Simulation Results

5.1. Case 1: Two-arm planar wheeled mobile manipulator

5.1.1. Simulation conditions. A two-link planar manipulator is mounted on a differentially driven mobile base at point F on the main axis of the base as shown in Fig. 2. All of the manipulator parameters and simulation conditions are

https://doi.org/10.1017/S0263574708004578 Published online by Cambridge University Press

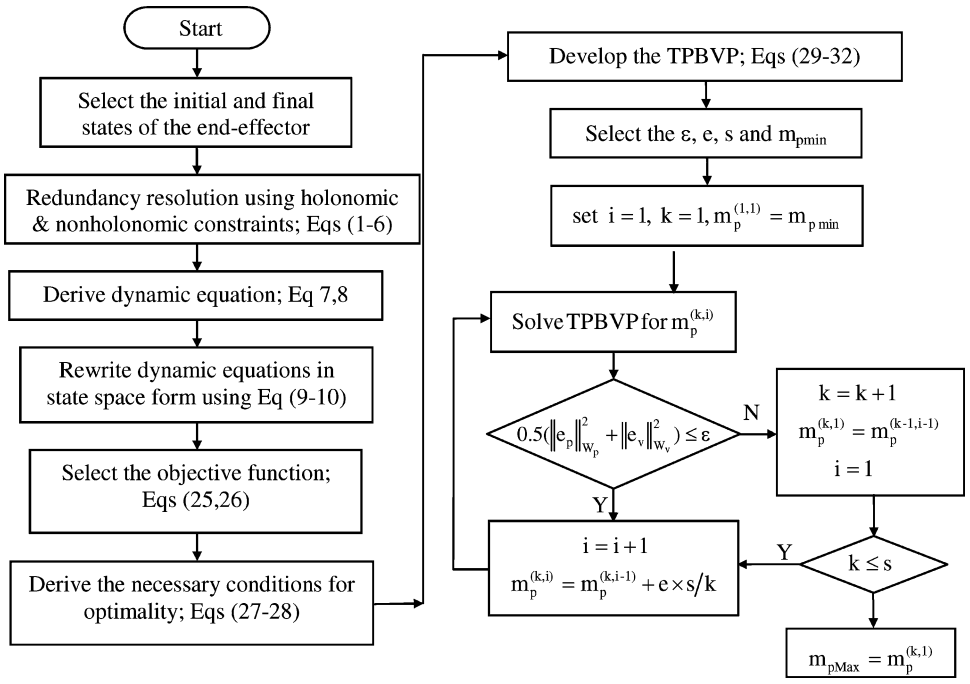

Fig. 1. Algorithm of maximum payload calculation.

the same used in ref. [13]. Suppose that L_0 is 40 cm. The links' parameters and their inertia properties are shown in Table I. The load must be carried from an initial point with coordinate ($x_e = 0.3$ m, $y_e = 0.5$ m) to the final point with coordinate ($x_e = 2.45$ m, $y_e = 0.5$ m) during the overall time $t_f = 1.9$ s, such that the maximum allowable load can be carried between these two points at the specified time. The inertia property of the payload is ignored, and it is assumed to be a point mass. It should be noted that final load position is not feasible without the base motion. Simultaneously, the mobile base is initially at point ($x_f = 0.75$ m, $y_f = 0.25$ m, $\theta_0 = 0$) and moves to final position ($x_f = 1.6$ m, $y_f = 0.5$ m). The actuator constants are given as follows:

$$K_1 = [34.67 \quad 12.21]^T \text{ N.m},$$
$$K_2 = \text{diag}(6.45 \quad 2.4)\,\text{N.m.s/Rad}$$

It must be noticed that the formulation presented for path planning of mobile manipulator in refs. [26]–[28] is not applicable here. Here the extra DOFs are solved using

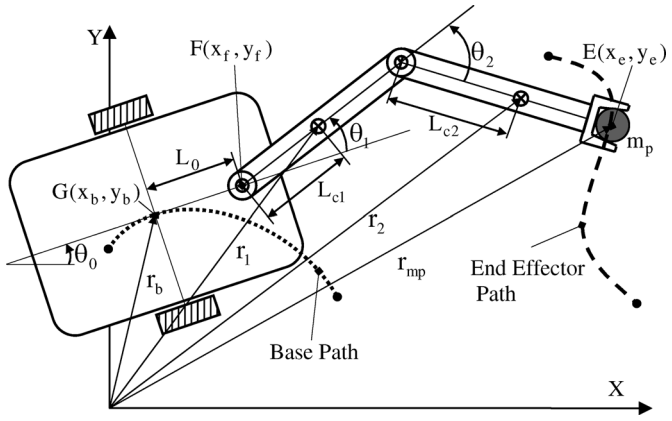

Fig. 2. Schematic view of wheeled mobile manipulator.

Table I. Links' parameters and inertia properties.

No	Length (m)	Mass (kg)	Moment of inertia (kg.m^2)			Link center of mass (m)
1	0.5	5	0	0	0	−0.25
			0	0.416	0	0
			0	0	0.416	0
2	0.5	3	0	0	0	−0.25
			0.0625	0	0	
			0	0	0.0625	0

holonomic constraints, so the generalized coordinates can be selected in such a way that the nonholonomic constraints do not appear in TPBVP directly. While in formulation obtained in refs. [26]–[28], the dynamic equations are directly dependent on nonholonomic constraints which increases the order of system and complicates the solution of TPBVP significantly.

5.1.2. Dynamics of the system. In order to define the mobile manipulator, the mechanical system generalized coordinates can be chosen as: $q = [q_b \;\; q_m] = [x_f \;\; y_f \;\; \theta_0 \;\; \theta_1 \;\; \theta_2]$, where $q_b = [x_f \;\; y_f \;\; \theta_0]$ are generalized coordinates of the mobile base and $q_m = [\theta_1 \;\; \theta_2]$ are the generalized coordinates of the arm as shown in Fig. 2. For this mobile manipulator the center of mass of the base, arms and payload can be obtained as follows:

$$\begin{aligned} r_b &= [x_f - L_0\cos(\theta_0) \quad y_f - L_0\sin(\theta_0)]^T \\ r_1 &= [x_f + L_{c1}\cos(\theta_{10}) \quad y_f + L_{c1}\sin(\theta_{10})]^T \\ r_2 &= [x_f + L_1\cos(\theta_{10}) + L_{c2}\cos(\theta_{210}) \quad y_f + L_1\sin(\theta_{10}) \\ &\quad + L_{c2}\sin(\theta_{210})]^T, \qquad (34) \\ r_{mp} &= [x_f + L_1\cos(\theta_{10}) + L_2\cos(\theta_{210}) \quad y_f + L_1\sin(\theta_{10}) \\ &\quad + L_2\sin(\theta_{210})]^T \end{aligned}$$

https://doi.org/10.1017/S0263574708004578 Published online by Cambridge University Press

where r_b, r_1, r_2, and $r_{mp}$are the center of mass vectors of the base, first link, second link, and payload respectively, L_{c1} and L_{c2} are the links center of mass, $\theta_{10} = \theta_0 + \theta_1$ and $\theta_{210} = \theta_0 + \theta_1 + \theta_2$. By differentiating Eqs. (34) with respect to time, velocity vectors can be obtained using which the total kinematic energy of the system can be calculated as follows:

$$K = 0.5\left(m_b\dot{r}_b^2 + m_1\dot{r}_1^2 + m_2\dot{r}_2^2 + m_p\dot{r}_{mp}^2\right) + 0.5\left(I_b\dot{\theta}_0^2 + I_1(\dot{\theta}_0 + \dot{\theta}_1)^2 + I_2(\dot{\theta}_0 + \dot{\theta}_1 + \dot{\theta}_2)^2\right), \quad (35)$$

where m_b, m_1, m_2, and m_p are the mass of base, first link, second link, and payload, I_b, I_1, and I_2 are the moment of inertia of base, first link, and second link, respectively. Because the mobile manipulator movement is in the horizontal plane, the potential energy is zero, therefore the Lagrangian is equal to kinematic energy, $L = K$. Now, using the Lagrange method, dynamic equations can be obtained as follows:

$$\begin{bmatrix} F_x \\ F_y \\ T_0 \\ U_1 \\ U_2 \end{bmatrix} = \begin{bmatrix} J_{11} & J_{12} & J_{13} & J_{14} & J_{15} \\ J_{12} & J_{22} & J_{23} & J_{24} & J_{25} \\ J_{13} & J_{23} & J_{33} & J_{34} & J_{35} \\ J_{14} & J_{24} & J_{34} & J_{44} & J_{45} \\ J_{15} & J_{25} & J_{35} & J_{45} & J_{55} \end{bmatrix} \begin{bmatrix} \ddot{x}_f \\ \ddot{y}_f \\ \ddot{\theta}_0 \\ \ddot{\theta}_1 \\ \ddot{\theta}_2 \end{bmatrix} + \begin{bmatrix} C_1 \\ C_2 \\ C_3 \\ C_4 \\ C_5 \end{bmatrix}, \quad (36)$$

where, J_{ij} $i, j = 1, \ldots, 5$ are functions of $q = [x_f \;\; y_f \;\; \theta_0 \;\; \theta_1 \;\; \theta_2]$ and C_i $i = 1, \ldots, 5$ are functions of q and $\dot{q}$. The details of these equations are given in Appendix.

The position of the end-effector in the world reference frame RF_w can be specified with x_e and y_e as shown in Fig. 2, therefore operational coordinated of the end-effector can be chosen as $p_{ee} = [x_e \;\; y_e]$ and the end-effector degrees of freedom in the Cartesian coordinate system will be $m = 2$. The system degree of freedom is equal to $n = 5$, hence the system has redundancy of order $R = n - m = 3$ and needs three additional kinematical constraints for proper coordination. Meanwhile, the mobile base has one nonholonomic constraint ($c = 1$) i.e., the rolling without slipping condition for the driven wheels,

$$\dot{x}_f \sin(\theta_0) - \dot{y}_f \cos(\theta_0) + L_0\dot{\theta}_0 = 0. \quad (37)$$

Hence, the number of kinematical constraints which must be applied to the system for redundancy resolution is equal to $r = R - c = 2$. In this case, with the previously specified base trajectory during the motion, the user-specified additional constraints can be considered as the base position coordinates at point $F(x_f, y_f)$, which gives

$$x_f = X_{1z}; \quad y_f = X_{2z}, \quad (38)$$

where X_{1z} and X_{2z} are functions in terms of time, and by differentiating them with respect to time, $\dot{x}_f$, $\dot{y}_f$, $\ddot{x}_f$ and $\ddot{y}_f$can also be obtained. A fifth-order polynomial function is considered for the base trajectory along a straight-line path from $(0.75, 0.2)$ to $(1.6, 0.5)$ during the overall time $t_f = 1.9$ s. Velocity at start and stop time is considered to be zero. From the base motion, $\dot{x}_f$ and $\dot{y}_f$ are known, so by discretizing the base path and using Eq. (37), the angular position and velocity of the base in kth point can be obtained as

$$\begin{aligned} \dot{\theta}_{0k} &= (\dot{y}_{fk}\cos(\theta_{0k}) - \dot{x}_{fk}\sin(\theta_{0k}))/L_0 \\ \theta_{0(k+1)} &= \theta_{0k} + h\dot{\theta}_{0k} \end{aligned}, \quad (39)$$

where h is the sample time. Here the initial base angle is considered to be zero, $\theta_0(0) = 0$, therefore final base angle will be obtained as $\theta_0(1.9) = 0.304$ Rad. Initial and final configuration of the base and end-effector has been specified; therefore the boundary conditions can be determined as

$$\begin{aligned} &\theta_1(0) = 1.554\,\text{rad}, \quad \theta_2(0) = 1.998\,\text{rad}, \quad \dot{\theta}_1(0) = 0, \\ &\dot{\theta}_2(0) = 0, \quad \theta_1(t_f) = -0.858\,\text{rad}, \quad \theta_2(t_f) = 1.09\,\text{rad}, \\ &\dot{\theta}_1(t_f) = 0, \quad \dot{\theta}_2(t_f) = 0. \end{aligned} \quad (40)$$

Now in Eq. (36), by considering the two last rows of equations associated with nonredundant part, and substituting the known variables $(x_f, y_f, \theta_0, \dot{x}_f, \dot{y}_f, \dot{\theta}_0, \ddot{x}_f, \ddot{y}_f, \ddot{\theta}_0)$ in it, as explained in Section 2.2, Eq. (36) is reduced to

$$\begin{bmatrix} U_1 \\ U_2 \end{bmatrix} = \begin{bmatrix} \bar{J}_{44} & \bar{J}_{45} \\ \bar{J}_{45} & \bar{J}_{55} \end{bmatrix} \begin{bmatrix} \ddot{\theta}_1 \\ \ddot{\theta}_2 \end{bmatrix} + \begin{bmatrix} \bar{R}_1 \\ \bar{R}_2 \end{bmatrix}, \quad (41)$$

where $\bar{J}_{ij}$ $i, j = 4, 5$ and $\bar{R}_i$ $i = 1, 2$ are

$$\begin{aligned} \bar{J}_{44} &= J_{44}; \quad \bar{J}_{45} = J_{45}; \quad \bar{J}_{55} = J_{55} \\ \bar{R}_1 &= J_{14}\ddot{x}_f + J_{24}\ddot{y}_f + J_{34}\ddot{\theta}_0 + C_4 \\ \bar{R}_2 &= J_{15}\ddot{x}_f + J_{25}\ddot{y}_f + J_{35}\ddot{\theta}_0 + C_5. \end{aligned} \quad (42)$$

$\bar{R}_i$ $i = 1, 2$are the functions of θ_1, θ_2, $\dot{\theta}_1$, $\dot{\theta}_2$, and t, so the state vectors can be defined as follows:

$$X_1 = \begin{bmatrix} \theta_1(t) \\ \theta_2(t) \end{bmatrix} = \begin{bmatrix} x_1(t) \\ x_3(t) \end{bmatrix}, \quad X_2 = \begin{bmatrix} \dot{\theta}_1(t) \\ \dot{\theta}_2(t) \end{bmatrix} = \begin{bmatrix} x_2(t) \\ x_4(t) \end{bmatrix}. \quad (43)$$

Using Eq. (10), the state space form of the dynamical equation of motion becomes

$$\begin{aligned} \dot{x}_1 &= x_2 \\ \dot{x}_2 &= P(\bar{\mathrm{J}}_{22}(\mathrm{U}_1 - \bar{\mathrm{R}}_1) - \bar{\mathrm{J}}_{12}(\mathrm{U}_2 - \bar{\mathrm{R}}_2)) \\ \dot{x}_3 &= x_4 \\ \dot{x}_4 &= P(-\bar{\mathrm{J}}_{12}(\mathrm{U}_1 - \bar{\mathrm{R}}_1) + \bar{\mathrm{J}}_{22}(\mathrm{U}_2 - \bar{\mathrm{R}}_2)), \end{aligned} \quad (44)$$

where $P = 1/(\bar{J}_{11}\bar{J}_{22} - \bar{J}_{12}^2)$. For this two-link mobile manipulator, the penalty matrices can be selected as follows:

$$W_1 = \mathrm{diag}(w_1, w_3); \; W_2 = \mathrm{diag}(w_2, w_4); \; R = \mathrm{diag}(r_1, r_2). \quad (45)$$

https://doi.org/10.1017/S0263574708004578 Published online by Cambridge University Press

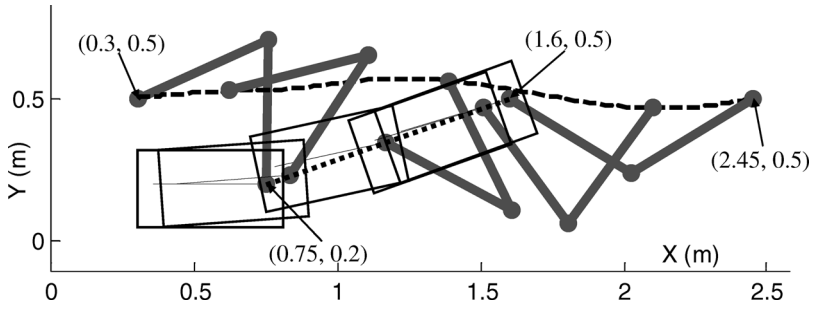

Fig. 3. Maximum payload trajectory.

To calculate the objective function, substituting Eq. (45) into Eq. (26) results in

$$L = 0.5 \times \left(r_1 u_1^2 + r_2 u_2^2 + w_1 x_1^2 + w_3 x_3^2 + w_2 x_2^2 + w_4 x_4^2\right). \tag{46}$$

Now, according to Eq. (28), by considering the costate vector as $\psi = [x_5 \;\; x_6 \;\; x_7 \;\; x_8]$, the Hamiltonian function can be expressed as

$$H = L + x_5 \dot{x}_1 + x_6 \dot{x}_2 + x_7 \dot{x}_3 + x_8 \dot{x}_4, \tag{47}$$

where L and $\dot{x}_i$, $i = 1, \ldots, 4$ can be substituted from Eqs. (46) and (44), respectively. Using Eq. (30), the costate equations can be obtained by differentiating the Hamiltonian function with respect to states as

$$\begin{aligned} \dot{x}_5 &= -\partial H/\partial x_1 = -(w_1 x_1 + x_6 f_{21} + x_8 f_{41}) \\ \dot{x}_6 &= -\partial H/\partial x_2 = -(w_2 x_2 + x_5 + x_6 f_{22} + x_8 f_{42}) \\ \dot{x}_7 &= -\partial H/\partial x_3 = -(w_3 x_3 + x_6 f_{23} + x_8 f_{43}) \\ \dot{x}_7 &= -\partial H/\partial x_4 = -(w_4 x_4 + x_7 + x_6 f_{24} + x_8 f_{44}) \end{aligned}, \tag{48}$$

where $f_{ij} = \partial \dot{x}_i / \partial x_j$ and $\dot{x}_i$ can be replaced by Eq. (44). Using Eq. (31), by differentiating the Hamiltonian with respect to control and setting the derivative equal to zero, control functions in the admissible interval, $U^- < U < U^+$, can be obtained as follows:

$$\begin{aligned} U_1 &= P(x_8 \bar{J}_{12} - x_6 \bar{J}_{22})/r_1 \\ U_2 &= P(x_6 \bar{J}_{12} - x_8 \bar{J}_{11})/r_2. \end{aligned} \tag{49}$$

Then, by applying motors torque limitation, the optimal control becomes

$$TU_i = \begin{cases} U_i^+ & U_i \geq U_i^+ \\ U_i & \text{othewise}; \quad i = 1, 2, \\ U_i^- & U_i \leq U_i^- \end{cases} \tag{50}$$

where the extremal bounds of control for each motor are

$$\begin{aligned} U_1^+ &= k_{11} - k_{12} x_2, \; U_1^- = -k_{11} - k_{12} x_2, \\ U_2^+ &= k_{21} - k_{22} x_4, \; U_2^- = -k_{21} - k_{22} x_4. \end{aligned} \tag{51}$$

Consequently, eight nonlinear ordinary differential equations are obtained by substituting Eqs. (50) and (51) into Eqs. (44) and (48), which with eight boundary conditions given in Eq. (40), construct a two-point boundary value problem.

The formulation of the problem is obtained, now using the algorithm presented in Fig. 1 simulation is performed. Accuracy values in payload calculation and TPBVP solution are considered to be $e = 0.1$ and $\varepsilon = 1e-4$, respectively. The initial values of the costate vector are considered to be zero, $\psi(0) = 0$ and the penalty matrices are chosen to be: $W_p = W_v = \text{diag}(1)$, $W_1 = [0]$, $W_2 = \text{diag}(0.01)$, and $R = \text{diag}(1e-5)$. At this condition, maximum payload is found to be 20.2 kg which has reasonable agreement with obtained maximum payload (21.92 kg) in ref. [13]. In this case study, the order of the equations is eight, and the runtime of the TPBVP solution is approximately 10 s using the computer with Pentium4, CPU 3GHz, and 512M of RAM. Since 8 to 10 iterations are required to achieve the final solution, the final runtime will be 100 s.

The obtained optimal path of the end-effector and the prespecified base path are shown in Fig. 3. This figure also demonstrates the system configurations at $t = 0$, $t_f/4$, $t_f/2$, $3t_f/4$, and t_f. The angular positions and velocities of joints are given in Figs. 4 and 5, respectively. Unlike the results obtained by iterative linear programming method[13] in which the boundary conditions have not been exactly satisfied (e.g., the angular position of the second joint has an error of about 8 degree and the angular velocity of the first joint has an error of about 14 degree/s), the results obtained in present paper do not have this problem and there is no error in satisfying the final boundary conditions. So the end-effector places in desired position accurately with zero velocity at final time, as shown in Figs. 4 and 5. Figures 6 and 7 are the optimal controls to carry the maximum payload, which also show the upper and lower bounds of the actuator torque capacity. By increasing the payload from $m_{p\min}$ to $m_{p\max}$, the required torque becomes more and torque curves lay on their own limits, until the payload reaches to its maximum value and motors operate at their maximum capacities.

5.2. *Case 2: Linear tracked PUMA*

A spatial three-jointed PUMA robot mounted on a linear tracked base is considered as shown in Fig. 8. All of the manipulator parameters are the same used in ref. [15]. D-H parameters and actuator constants are given in Tables II and III. Suppose that initially the point-mass load is at a point with coordinates $p_0(x_e = 0.5\,\text{m}, y_e = 0, z_e = -0.1\,\text{m})$ and it must reach to final point with coordinates $p_f(x_e = 0, y_e = 1.2\,\text{m},$

https://doi.org/10.1017/S0263574708004578 Published online by Cambridge University Press

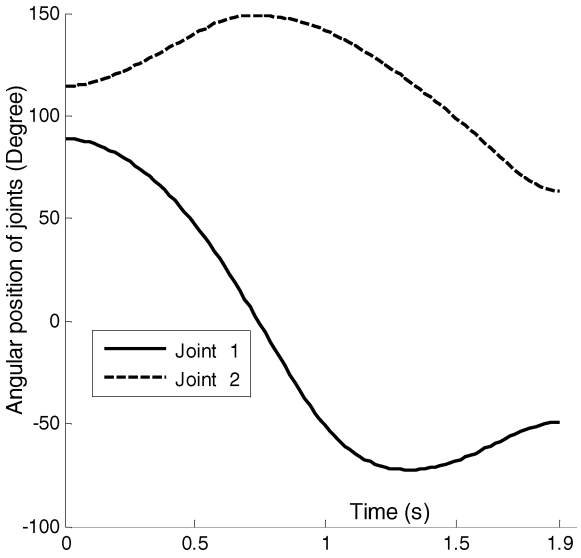

Fig. 4. Angular positions of joints.

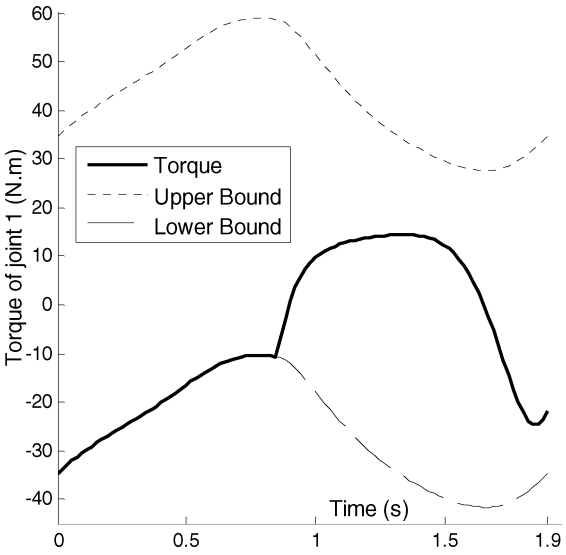

Fig. 6. Actuator torque at first joint.

$z_e = 1.04\,\text{m})_f$ at $t_f = 2.4\,\text{s}$. The base mass is assumed to be 21 kg and the manipulator characteristics are shown in Table IV.

In this case, the generalized coordinates can be considered as $q = [\,q_1\ \theta_1\ \theta_2\ \theta_3\,]$, where q_1 is the linear motion of the mobile base and $\theta_1, \theta_2, \theta_3$ are the links angles. The end-effector degrees of freedom in the Cartesian coordinate system is $m = 3$ and the system degree of freedom is equal to $n = 4$, hence the system has 1 degree of redundancy and needs one additional kinematical constraint for redundancy resolution. For this purpose, the base is considered to move with the prespecified rest-to-rest motion as a fifth-order polynomial function from $x_{bi} = 0$ to $x_{bf} = 0.437\,\text{m}$ during the overall time $t_f = 2.4\,\text{s}$. Consequently, the boundary conditions can be determined as

$$q_{nr}(0) = [0, 0, 90^\circ],\ q_{nr}(t_f) = [90^\circ,\ 45^\circ,\ -10^\circ],$$
$$\dot{q}_{nr}(0) = \dot{q}_{nr}(t_f) = [0,\ 0,\ 0].$$

According to the algorithm presented in Fig. 1, the initial payload value, initial values of costate vector, accuracy values, and penalty matrices are considered as follows:

$$m_{p\,\min} = 2\,\text{kg},\ \psi(0) = 0,\ e = 0.1,\ \varepsilon = 1e-4,$$
$$W_p = W_v = \text{diag}(1),\ W_1 = [0],$$
$$W_2 = \text{diag}(0.2),\ \text{and}\ R = \text{diag}(1e-3).$$

At this condition, maximum payload is found to be 12.6 kg. Figure 9 shows the optimal trajectory of mobile manipulator in Cartesian space. The end-effector movement starts from point (0.5, 0, -0.1) and ends at point (0, 1.2, 1.04). In this motion, the first link in addition to rotating 90° about own axis, translates 0.437 m along the axis Y.

$m_{p\,\max} = 12.6\,\text{kg}$ is the maximum payload for the considered penalty matrices, while by choosing the other penalty matrices, the other optimal trajectories with different specifications can be obtained. To illustrate this aspect,

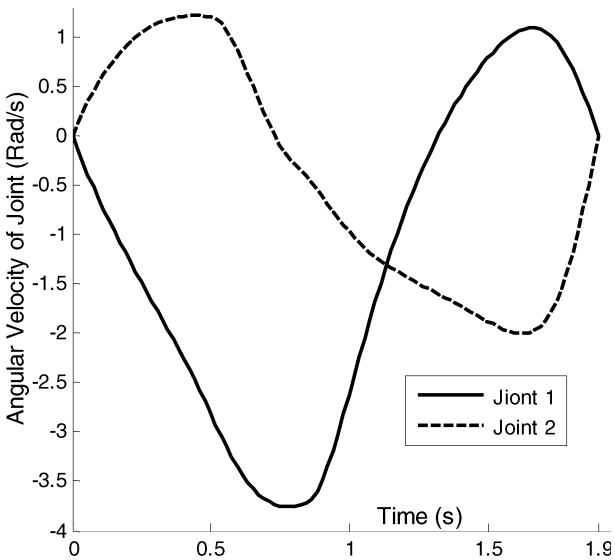

Fig. 5. Angular velocities of joints.

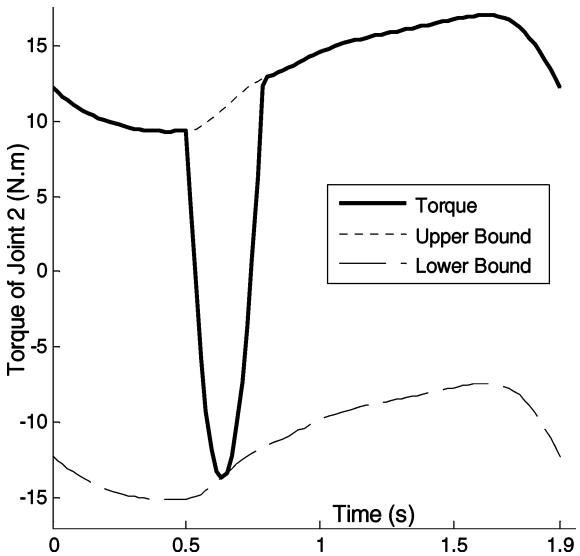

Fig. 7. Actuator torque at second joint.

https://doi.org/10.1017/S0263574708004578 Published online by Cambridge University Press

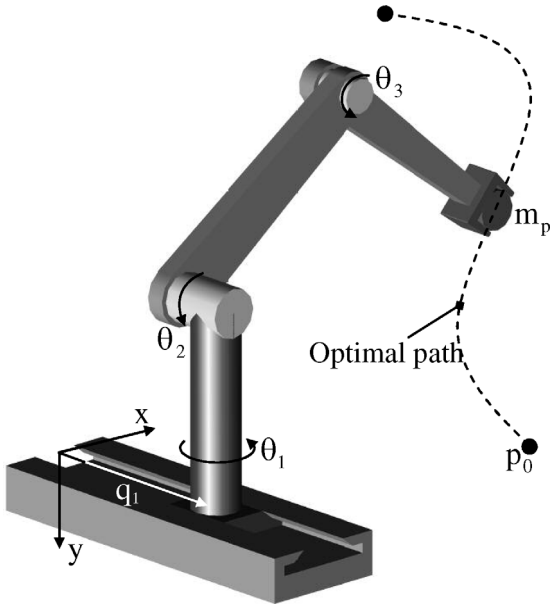

Fig. 8. A view of linear tracked mobile PUMA manipulator.

simulation is performed for $W_2 = \text{diag}(0.05)$. The other penalty matrices remain the same. In this case, the maximum payload is obtained to be 14 kg. The angular positions and velocities of joints for these two cases are given in Figs. 10 and 11, respectively. As expected, decreasing the W_2 increases the magnitude of angular velocities and constructs the other optimal path. Designer can select each of the obtained optimal paths depends on the limitation on angular velocities. The actuator torque and force are shown in Figs. 12(a)–12(d). As it can be seen in Fig. 12, the actuator curves in three joints are saturated and the mobile base force is tangent to its upper bound. Therefore the base actuator capacity determines the maximum payload value. In this case study, the order of the equations is 12, and the runtime of the TPBVP solution is approximately 16 s.

5.3. Case 3: Time-optimal control

In this section, at first, the effect of final time t_f on the maximum payload value is studied. Then, the time-optimal control is solved for a two-link manipulator and

Table II. D-H parameters.

No.	θ_i	α_i	$(m)a_i$	$(m)d_i$
Base	0	$\pi/2$	0	q_1
1	θ_1	$\pi/2$	0	0.4
2	θ_2	0	0.5	0
3	θ_3	0	0.5	0

Table III. Actuators constants.

No.	τ_{si}	ω_{si}	k_{1i}	k_{2i}
Base	40.62	6.6	40.62	6.15
1	10	5.71	10	1.75
2	30	6.41	30	4.68
3	6.67	4.6	6.67	1.45

Table IV. Links' parameters and inertia properties.

No	Length (m)	Mass (kg)	Moment of inertia (kg m^2)			Link center of mass (m)
1	0.4	12	0	0	0	0
			0	0.2	0	−.2
			0	0	0	0
2	0.5	10	0	0	0	−0.25
			0	0.2	0	0
			0	0	0.2	0
3	0.5	5 0	0	0	−0.25	
			0	0.1	0	0
			0	0	0.1	0

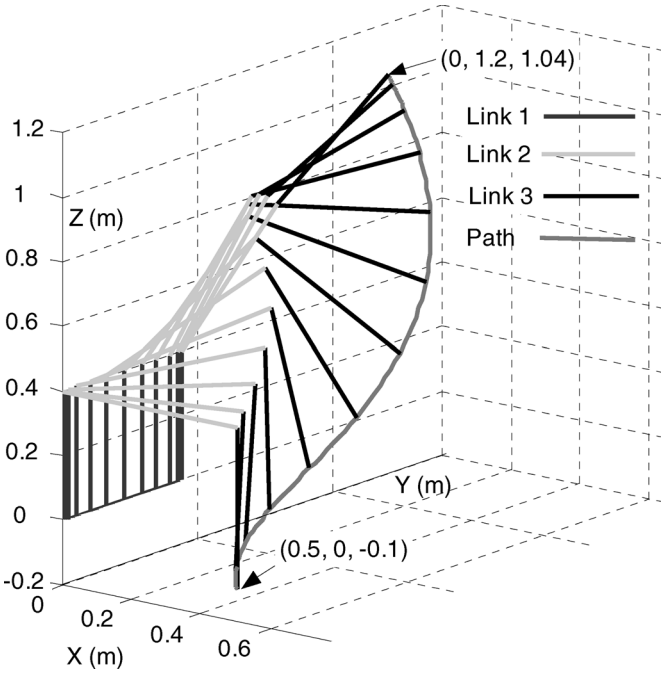

Fig. 9. Optimal trajectory of base, links, and end-effector.

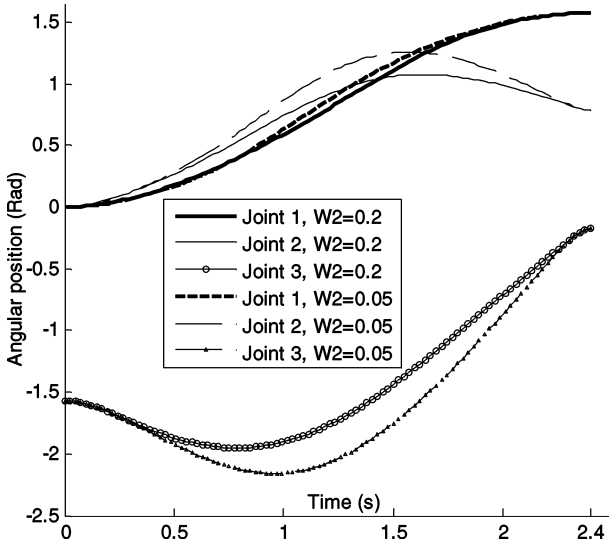

Fig. 10. Angular positions of joints.

https://doi.org/10.1017/S0263574708004578 Published online by Cambridge University Press

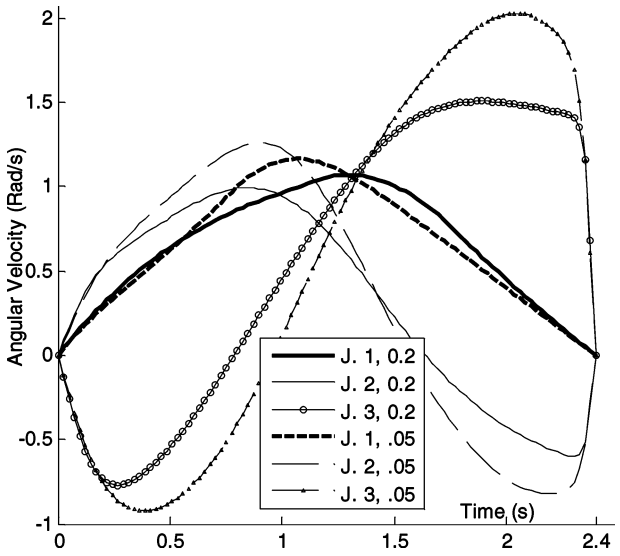

Fig. 11. Angular velocities of joints.

Table V. Maximum payloads for different final times.

Final time t_f (s)	1.083	1.2	1.4
$m_{p\max(\mathrm{Kg})}$	6	11.2	22.8

the result is compared with that obtained in ref. [22]. All the manipulator parameters and the boundary conditions are the same used in ref. [22]. The penalty matrices are selected as: $W_1 = W_2 = 0$, $R = diag(1)$. The obtained maximum payloads and the corresponding final times are given in Table V. As expected, by increasing the final time, the obtained maximum payload value is increased. Increasing the duration time reduces the acceleration and velocity of the system which leads to less acceleration, centrifugal and Coriolis forces, and more maximum payload.

Now, by setting the payload value equal to 6 kg and the maximum final time equal to 1.5 s, time-optimal control problem is solved using the same approach used to find the maximum payload trajectory. Step by step, final time

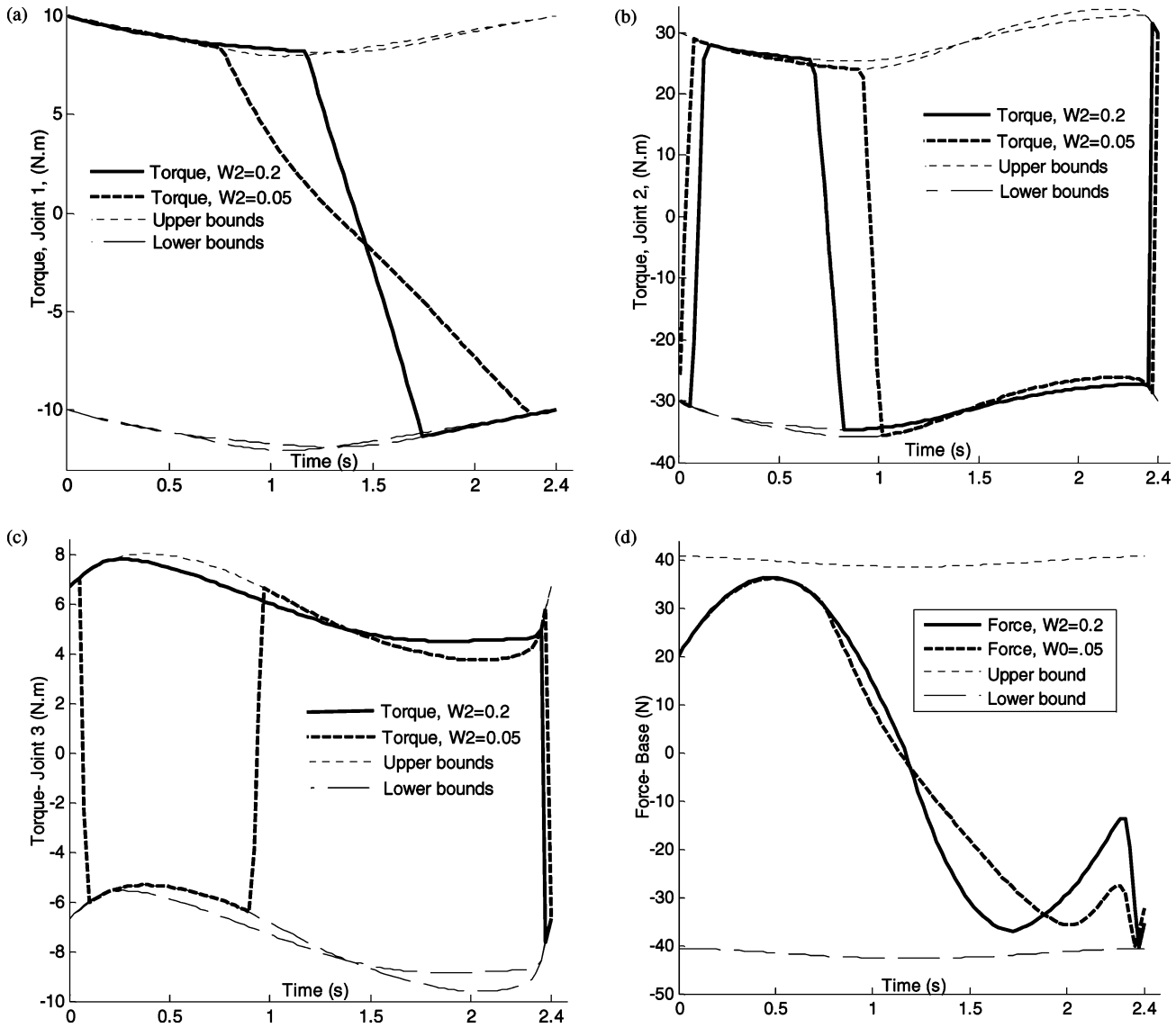

Fig. 12. (a) Actuator torque at first joint. (b) Actuator torque at second joint. (c) Actuator torque at third joint. (d) Actuator torque at base.

https://doi.org/10.1017/S0263574708004578 Published online by Cambridge University Press

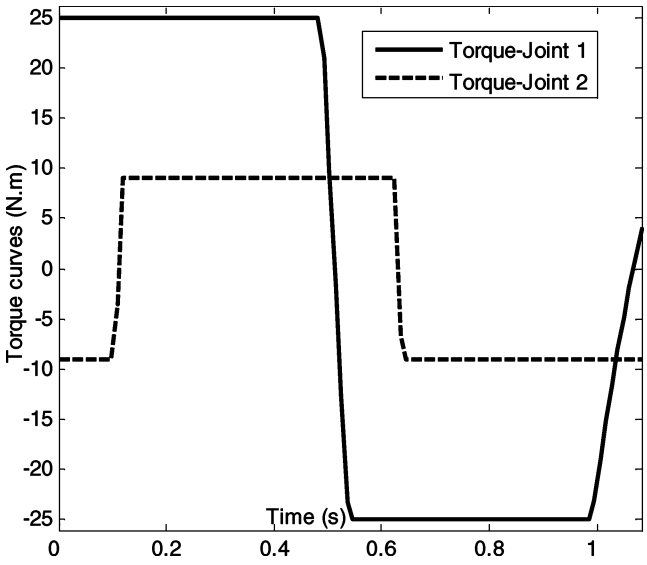

Fig. 13. Optimal controls, U_1 and U_2.

decreases and the TPBVP is solved according to the algorithm given in Fig. 1. In this case, the minimum time is found to be 1.083 s. The optimal controls are shown in Fig. 13, and the optimal states are shown in Fig. 14. The obtained minimum time, angular positions and velocities, and switch times in controls are the same obtained in ref. [22]. As it can be seen in Fig. 13, control switching between the upper and lower bound occurred with a finite rate, while the controls in ref. [22] switch immediately with an infinite rate.

6. Contribution

In all the previous works dealing with maximum payload calculation, direct methods are used to solve the path-planning problem. In this paper, indirect method is employed as an exact and powerful method which explicitly solves the optimization problem. Optimality conditions for carrying the maximum payload in point-to-point motion are derived using the Pontryagin's minimum principle. The obtained conditions lead to a bang-bang control with $4m$ ordinary differential equations, one algebraic equation, and $4m$ boundary conditions. By solving these equations, maximum payload and corresponding optimal path can be obtained directly. But bang-bang control results in infinite jerk in system, and also the presence of algebraic equation makes the problem solution difficult. So, formulation is improved, and an algorithm is developed to convert the optimization problem into a standard form of TPBVP which is easily solved with bvp4c commands in MATLAB.

In the proposed method, the generalized coordinates and additional kinematic constraints are selected in such a way that the system's motion coordination is guaranteed and the nonholonomic constraints do not appear in TPBVP directly, unlike the method given in refs. [26]–[28]. Here, the complete form of the obtained nonlinear equation is used, and unlike the previous works, linearizing the equations,[5,13–16] using of a fixed-order polynomial as the solution form,[8–12] or developing the additional numerical algorithm to solve the problem[20–22,26–28] is not required. Also calculation of Hamiltonian's derivatives with respect to the system variables is a simple and straightforward task unlike the complicated procedures needed to derive the equations in spline[8] and ILP[13] methods.

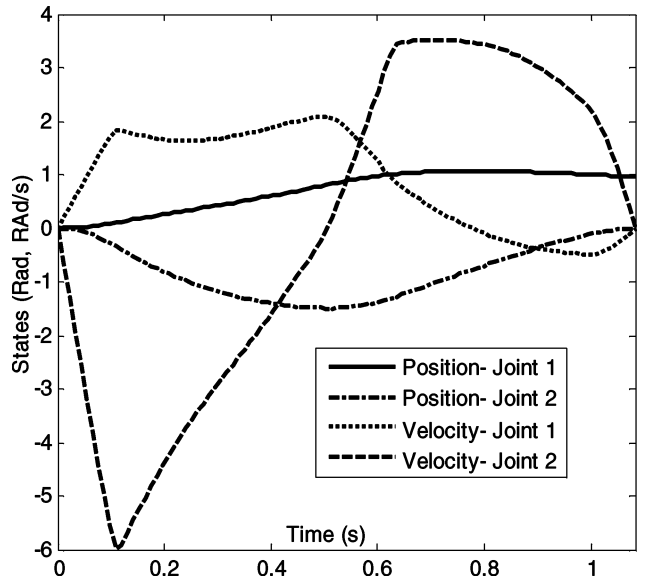

Fig. 14. Time-optimal states, X_i, $i = 1 \ldots 4$.

7. Conclusion

Three simulation studies are presented to investigate the application of the proposed approach. In the first simulation for a two-link wheeled mobile manipulator, the procedure of obtaining the equations are given in detail. The maximum payload in this method is found to be 20.2 kg which has reasonable agreement with result obtained by ILP method in ref. [13] (21.92 kg). In optimal control method, boundary conditions are satisfied exactly, while the results obtained by ILP method have a considerable error in final time. In another simulation, a three-link manipulator mounted on a linear tracked base is considered. It is shown that, we are able to have various maximum payload trajectories with different characteristics via considering the different objective function. It means that in addition to maximizing the payload, other objectives such as angular velocity or applied torque can be minimized. It is also seen that the runtime of the problem solution does not increase with problem size significantly. In the last case study, the effect of final time on the maximum payload is investigated. It is shown that increasing the final time leads to increase in the maximum payload value. Finally, the algorithm presented is applied to solve the time-optimal control problem. The obtained optimal control leads to the quasi bang-bang control which is very close to the result reported in ref. [22].

References

1. C. Cosma, M. Confente, M. Governo and R. Fiorini, "An autonomous robot for indoor light logistics," *Proceedings of the IEEE International Conference on Intelligent Robots and Systems* Sendai Japan 3, pp. 3003–3008 (2004).

https://doi.org/10.1017/S0263574708004578 Published online by Cambridge University Press

2. T. L. Huntsberger, "Autonomous multi-rover system for complex planetary retrieval operations," *Proceedings of the SPIE Symposium on Sensor Fusion and Decentralized Control in Autonomous Robotic Agents*, Boston 3209 (1997) pp. 220–229.
3. H. Seraji, "A unified approach to motion control of mobile manipulators," *Int. J. Robot. Res.* **17**(12), 107–118 (1998).
4. L. T. Wang and B. Ravani, "Dynamic load carrying capacity of mechanical manipulators-Part 1," *Trans. ASME, J. Dyn. Syst. Meas. Control* **110**, 46–52 (1988).
5. L. T. Wang and B. Ravani, "Dynamic load carrying capacity of mechanical manipulators-Part 2," *Trans. ASME, J. Dyn. Syst. Meas. Control* **110**, 53–61 (1988).
6. T. Chettibi, H. E. Lehtihet, M. Haddad and S. Hanchi, "Minimum cost trajectory planning for industrial robots," *Eur. J. Mech.,* A/Solids **23**, 703–715 (2004).
7. D. G. Hull, "Conversion of optimal control problems into parameter optimization problems," *J. Guid. Control Dyn.* **20**(1), 57–60 (1997).
8. C-Y. E Wang, W. K. Timoszyk and J. E. Bobrow, "Payload maximization for open chained manipulator: Finding motions for a Puma 762 robot," *IEEE Trans. Robot. Autom.* **17**(2), 218–224 (2001).
9. Xin-Sheng Ge and Li-Qun Chen, "Optimal motion planning for nonholonomic systems using genetic algorithm with wavelet approximation," *Appl. Math. Comput.* **180**, 76–85 (2006).
10. M. Haddad, T. Chettibi, S. Hanchi and H. E. Lehtihet, "Optimal motion planner of mobile manipulators in generalized point-to-point task," *9th IEEE International Workshop on Advanced Motion Control*, Istanbul (2006) pp. 300–306.
11. A. Kelly and B. Nagy, "Reactive nonholonomic trajectory generation via parametric optimal control," *Int. J. Robot. Res.* **22**(8), 583–601 (2003).
12. E. Papadopoulos, I. Poulakakis and I. Papadimitriou, "On path planning and obstacle avoidance for nonholonomic platforms with manipulators: A polynomial approach," *Int. J. Robot. Res.* **21**(4), 367–383 (2002).
13. M. H. Korayem and H. Ghariblu, "Maximum allowable load of mobile manipulator for two given end points of end-effector," *Int. J. Adv. Manuf. Technol.* **24**(10), 743–751 (2004).
14. M. H. Korayem and H. Gariblu, "Maximum allowable load on wheeled mobile manipulators imposing redundancy constraints," *Robot. Auton. Syst.* **44**, 151–159 (2003).
15. M. H. Korayem and H. Gariblu, "Analysis of wheeled mobile flexible manipulator dynamic motions with maximum load carrying capacities," *Robot. Auton. Syst.* **48**(3), 63–76 (2004).
16. H. Gariblu and M. H. Korayem, "Trajectory optimization of flexible mobile manipulators," *Robotica* **24**(3), 333–335 (2006).
17. J. Arora, *Introduction to Optimum Design* (Second Edition, Elsevier, Academic Press, 2004).
18. D. E. Kirk, *Optimal Control Theory, An Introduction* (Englewood Cliffis New Jersey, 1970).
19. Z. Shiller and S. Dubowsky, "Robot path planning with obstacles, actuators, gripper and payload constraints," *Int. J. Robot. Res.* **8**(6), 3–18 (1986).
20. W. Szyszkowski and R. Fotouhi, "Improving time-optimal control maneuvers of two-link robotic manipulators," *J. Guid. Control Dyn.* **23**(5), 888–889 (2000).
21. Z. Shiller, "Time-energy optimal control of articulated systems with geometric path constraints," *Proceedings of the IEEE International Conference on Robotics and Automation*, San Diego, CA USA (1994) Vol. 4, pp. 2680–2685.
22. R. Fotouhi and W. Szyszkowski, "An algorithm for time optimal control problems," *J. Guid. Control Dyn.* **120**, 414–418 (1998).
23. G. Bessonnet and S. Chessé, "Optimal dynamics of actuated kinematic chains, Part 2: Problem statements and computational aspects," *Eur. J. Mech.,* A/Solids **24**, 472–490 (2005).
24. E. Bertolazzi, F. Biral and M. Da Lio, "Symbolic–numeric indirect method for solving optimal control problems for large multibody systems," *Multibody System Dynamics* **13**(2), 233–252 (2005).
25. M. R. Sentinella and L. Casalino, "Genetic algorithm and indirect method coupling for low-thrust trajectory optimization", *42nd AIAA/ASME/SAE/ASEE Joint Propulsion Conference & Exhibit*, California (2006).
26. A. Mohri, S. Furuno, M. Iwamura and M. Yamamoto, "Sub-optimal trajectory planning of mobile manipulator," *Proceedings of the IEEE International Conference on Robotics and Automation*, Seoul, Korea (2001) pp. 1271–1276.
27. A. Mohri, S. Furuno and M. Yamamoto, "Trajectory planning of mobile manipulator with end-effector's specified path," *Proceedings of the IEEE International Conference on Intelligent Robots and Systems* Maui, HI, USA (2001) pp. 2264–2269.
28. S. Furuno, M. Yamamoto and A. Mohri, "Trajectory planning of mobile manipulator with stability considerations," *Proceedings of the IEEE International Conference on Robotics and Automation*, Taipei, Taiwan (2003) pp. 3403–3408.
29. A. Ghasempoor and N. Sepehri, "A measure of stability for mobile based manipulators," *Proceedings of the IEEE International Conference on Robotics and Automation*, Nagoya, Japan (1995) pp. 2249–2254.
30. D. A. Rey and E. G. Papadopoulos, "Online automatic tip-over prevention for mobile and redundant manipulators," *Proceedings of the IEEE International Conference on Intelligent Robots and Systems*, Grenoble, France (1997) pp. 1273–1278.

Appendix

$$
\begin{aligned}
a_1 &= m_p L_2 + m_2 L_{c2}, \quad a_2 = m_p L_1 L_2 + m_2 L_1 L_{c2},\\
a_3 &= m_p L_1 + m_2 L_1 + m_1 L_{c1},\\
J_{11} &= J_{22} = m_b + m_1 + m_2 + m_p, \quad J_{12} = 0,\\
J_{13} &= m_b L_0 \sin(\theta_0) - (m_p L_1 + m_2 L_1 + m_1 L_{c1}) \sin(\theta_0 + \theta_1)\\
&\quad - a_1 \sin(\theta_0 + \theta_1 + \theta_2),\\
J_{14} &= -a_3 \sin(\theta_0 + \theta_1) - a_1 \sin(\theta_0 + \theta_1 + \theta_2),\\
J_{15} &= -a_1 \sin(\theta_0 + \theta_1 + \theta_2),\\
J_{23} &= -m_b L_0 \cos(\theta_0) + a_3 \cos(\theta_0 + \theta_1)\\
&\quad + a_1 \cos(\theta_0 + \theta_1 + \theta_2),\\
J_{24} &= a_3 \cos(\theta_0 + \theta_1) + a_1 \cos(\theta_0 + \theta_1 + \theta_2),\\
J_{25} &= a_1 \cos(\theta_0 + \theta_1 + \theta_2),\\
J_{33} &= m_b L_0^2 + m_2 L_{c2}^2 + m_1 L_{c1}^2 + m_2 L_1^2 + m_p L_2^2 + m_p L_1^2\\
&\quad + 2a_2 \cos\theta_2 + I_1 + I_2 + I_b,\\
J_{34} &= 2a_2 \cos\theta_2 + m_p L_2^2 + m_1 L_{c1}^2 + m_2 L_1^2 + m_2 L_{c2}^2\\
&\quad + m_p L_1^2 + I_2 + I_1,\\
J_{35} &= I_2 + a_2 \cos\theta_2 + m_p L_2^2 + m_2 L_{c2}^2,\\
J_{44} &= 2a_2 \cos\theta_2 + I_1 + I_2 + m_p L_1^2 + m_p L_2^2 + m_2 L_{c2}^2\\
&\quad + m_1 L_{c1}^2 + m_2 L_1^2,\\
J_{45} &= m_2 L_{c2}^2 + m_p L_2^2 + I_2 + a_2 \cos\theta_2,\\
J_{55} &= I_2 + m_p L_2^2 + m_2 L_{c2}^2.
\end{aligned}
$$

https://doi.org/10.1017/S0263574708004578 Published online by Cambridge University Press